Supplementary Information for "Extreme coastal El Niño events are tightly linked to the development of the Pacific Meridional Modes"

Cristian Martinez-Villalobos[1,2], Boris Dewitte[3,4,5], and René D. Garreaud[6]

[1]Facultad de Ingeniería y Ciencias, Universidad Adolfo Ibáñez
[2]Data Observatory Foundation, ANID Technology Center No. DO210001
[3]Centro de Estudios Avanzados en Zonas Áridas
[4]Facultad de Ciencias del Mar, Universidad Católica del Norte
[5]CECI, Université de Toulouse
[6]Departamento de Geofísica, Universidad de Chile

1 Text S1: Linear and Nonlinear Inverse Models

To test the patterns obtained and the evolution of events, we fitted three versions of inverse models to the data. The simplest one is a version of a linear inverse model (LIM) (Penland and Sardeshmukh 1995) given by

$$\frac{dx_i}{dt} = M_{ij}^{lin} x_j + B_{in}^{lin} \eta_n, \tag{1}$$

where identically to the case presented in the main text (see Methods) x_i represents each of the variables of interest, $M_{ij}^{lin} x_j$ the linear approximation to the deterministic dynamics, and $B_{in}^{lin} \eta_n$ the stochastic forcing of the system. The second model adds a quadratic nonlinearity, but neglects the interaction terms and it is given by

$$\frac{dx_i}{dt} = M_{ij}^{*} x_j + C_{ik}^{*}(x_k^2 - \langle x_k^2 \rangle) + B_{in}^{*} \eta_n. \tag{2}$$

The third model, which is the one primarily used throughout the paper (see equation 2 in the Methods section), includes the interaction terms and it is given by

$$\frac{dx_i}{dt} = M_{ij} x_j + C_{ikl}(x_k x_l - \langle x_k x_l \rangle) + B_{in} \eta_n. \tag{3}$$

The first model includes 6 predictors, the second one 12 (nonlinear v1), and the third model 27 (nonlinear v2). Other than the fact that the linear model only generates symmetric statistics between Coastal El Niño and Coastal La Niña events, we find that the three models generate highly consistent statistics of the evolution of the events, precipitation associated, and spatial patterns (Figs. S8 and S9).

2 Supplementary Figures

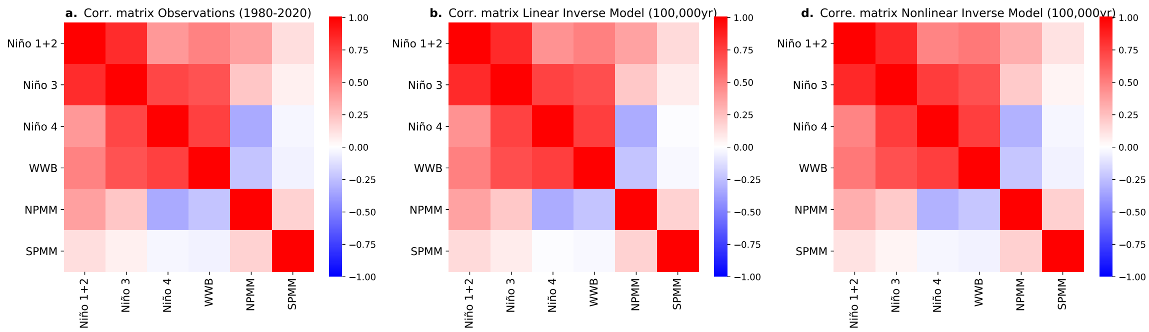

Figure S1: Correlation matrix between the main variables considered (Niño $1+2$, Niño 3, Niño 4, WWB, NPMM, SPMM indices) in **a.** observations (1980-2020) and simulated by a **b.** linear inverse model (eq. 1 in Text S1), and **c.** nonlinear inverse model (eq. 3 in Text S1).

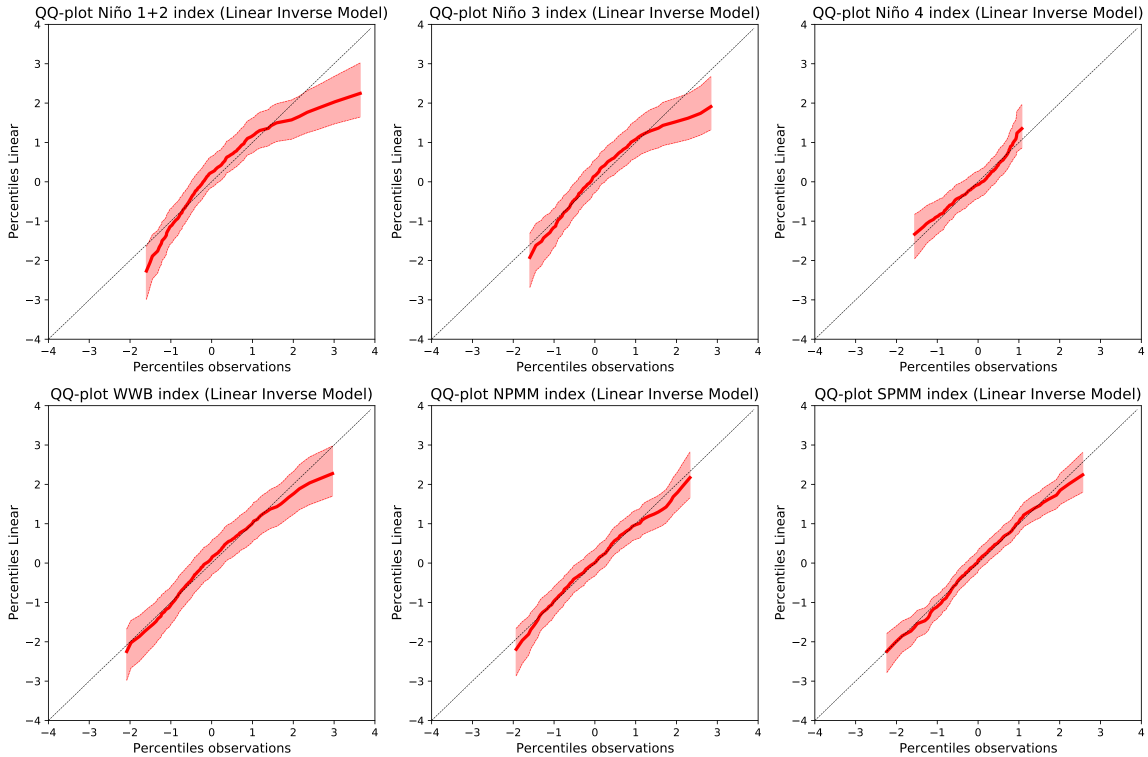

Figure S2: QQ-plots showing the observed (x-axis) and linear inverse model simulated (y-axis) 1st to 99th percentiles of the Niño 1+2, Niño 3, Niño 4, WWB, NPMM, and SPMM indices. The shading encompasses the 5th to 95th percentiles of modeled percentiles based on 2439 periods of the same length as observations (41 years) within the 100,000 years of simulated data.

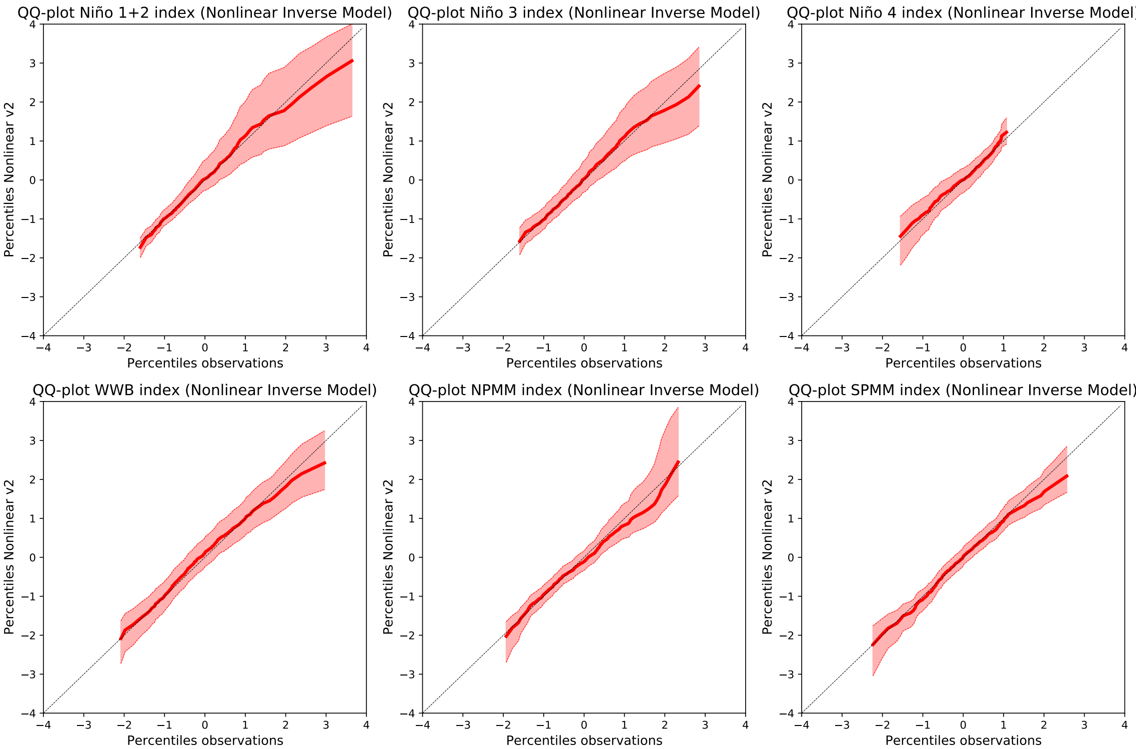

Figure S3: Same as Fig. S2 but using output from the nonlinear inverse model.

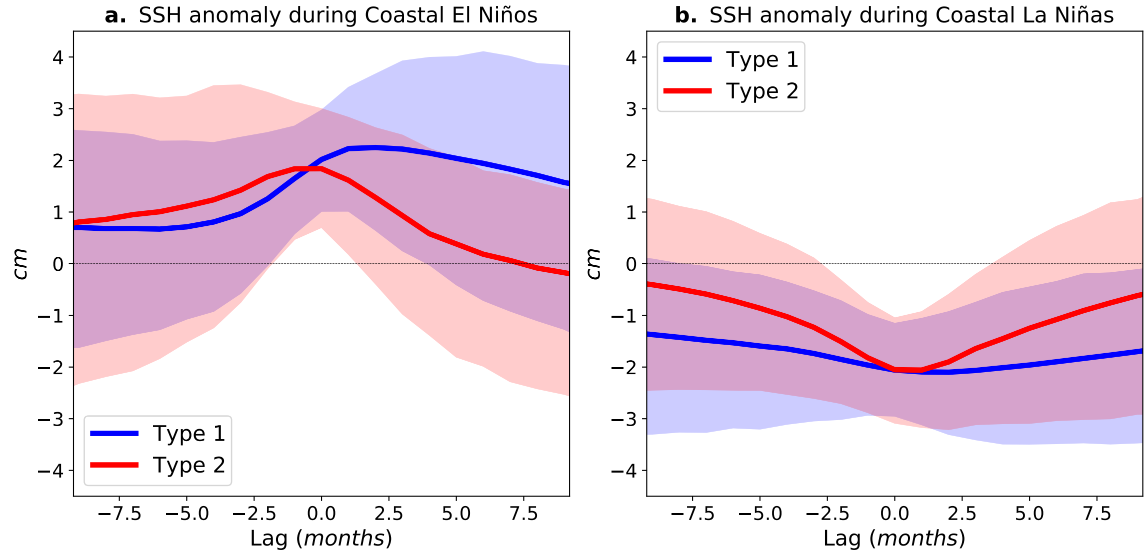

Figure S4: **a.** Evolution of the average sea surface height anomaly (SSHA) over the Niño 1+2 region nine months before to nine months after the peak of type-1 (blue) and type-2 (red) coastal El Niño events from the NLIM simulation. The shading denotes estimates of the 25th-75th percentile range of the SSHA evolution across events. **b.** Same as **a** but for coastal La Niña events.

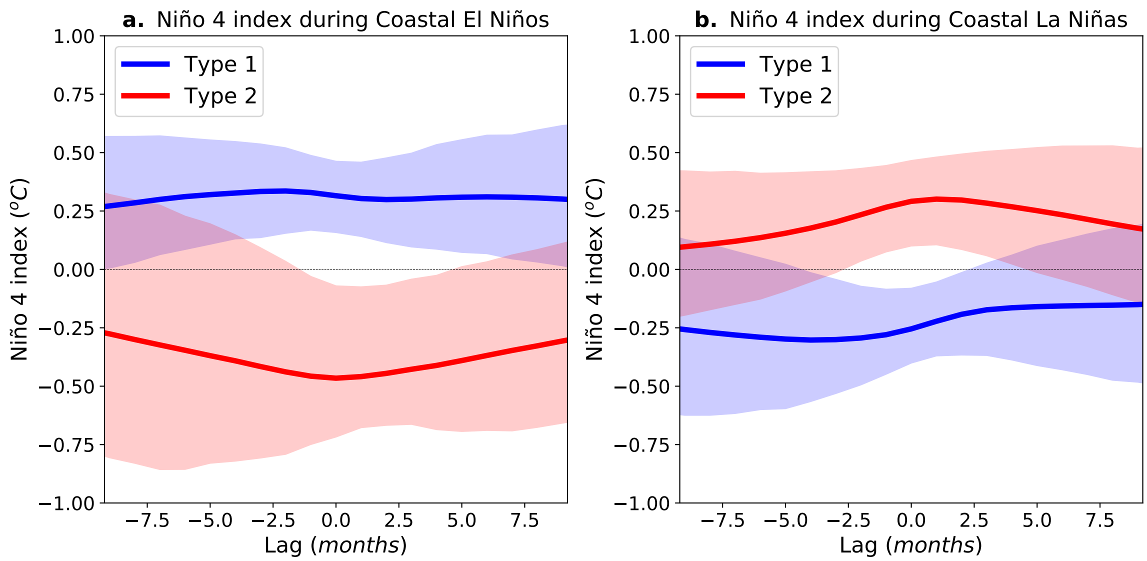

Figure S5: **a.** Evolution of the Niño 4 index nine months before to nine months after the peak of type-1 (blue) and type-2 (red) coastal El Niño events from the NLIM simulation. The shading denotes estimates of the 25th-75th percentile range of the index evolution. **b.** Same as **a** but for coastal La Niña events.

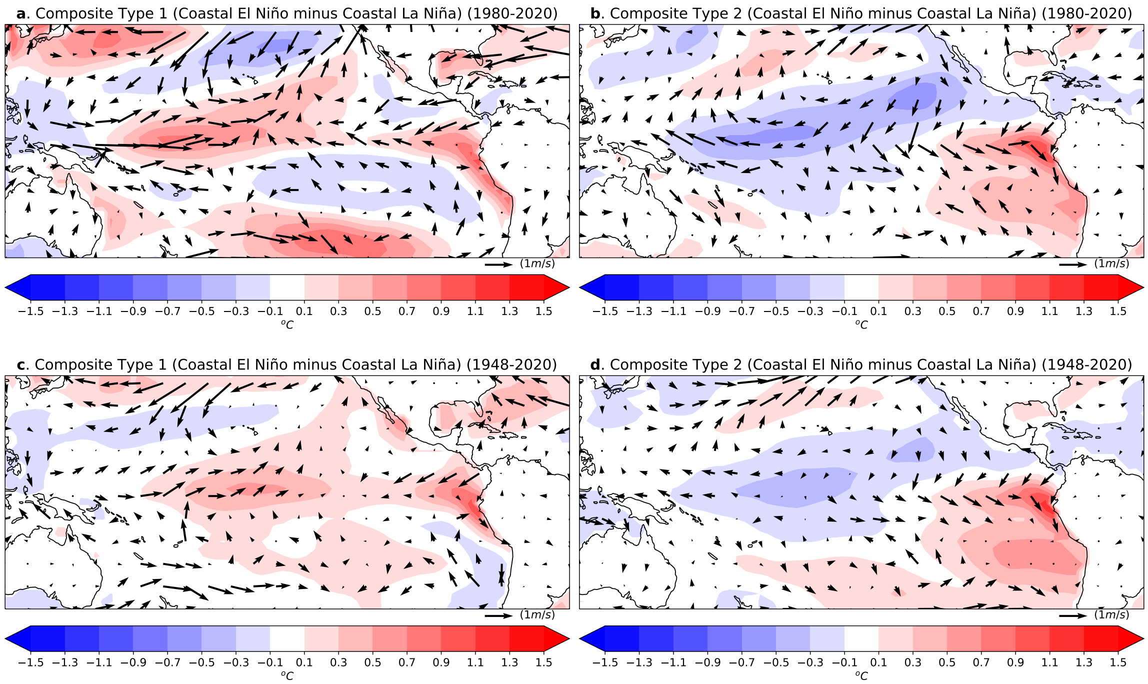

Figure S6: **a.** Sea surface temperature and wind anomalies composite of type-1 coastal El Niño minus coastal La Niña events during 1980-2020 (3 events: 1 warm, 2 cold). **b.** Sea surface temperature and wind anomalies composite of type-2 coastal El Niño minus coastal La Niña events during 1980-2020 (7 events: 2 warm, 5 cold). **c.** Same as **a** but for 1948-2020 (7 events: 3 warm, 4 cold). **d.** Same as **b** but for 1948-2020 (11 events: 3 warm, 8 cold). In this figure... COMPLETAR

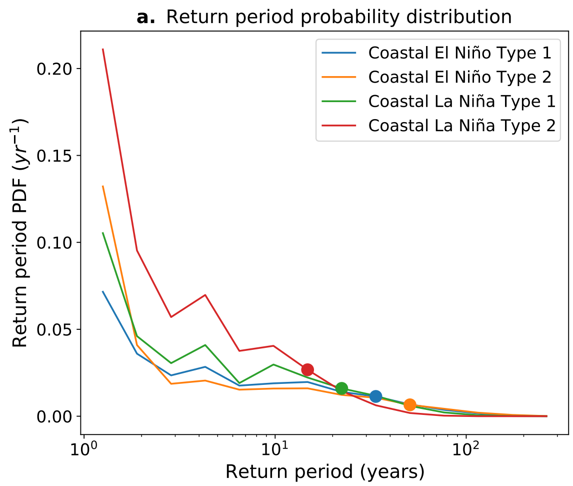

Figure S7: Probability distribution of return periods (duration of interval between events) of different types of coastal events in the NLIM simulation. In all cases short return periods are more frequent, with a long tail for extreme return periods. The circles denote the "average" return period of each type of event.

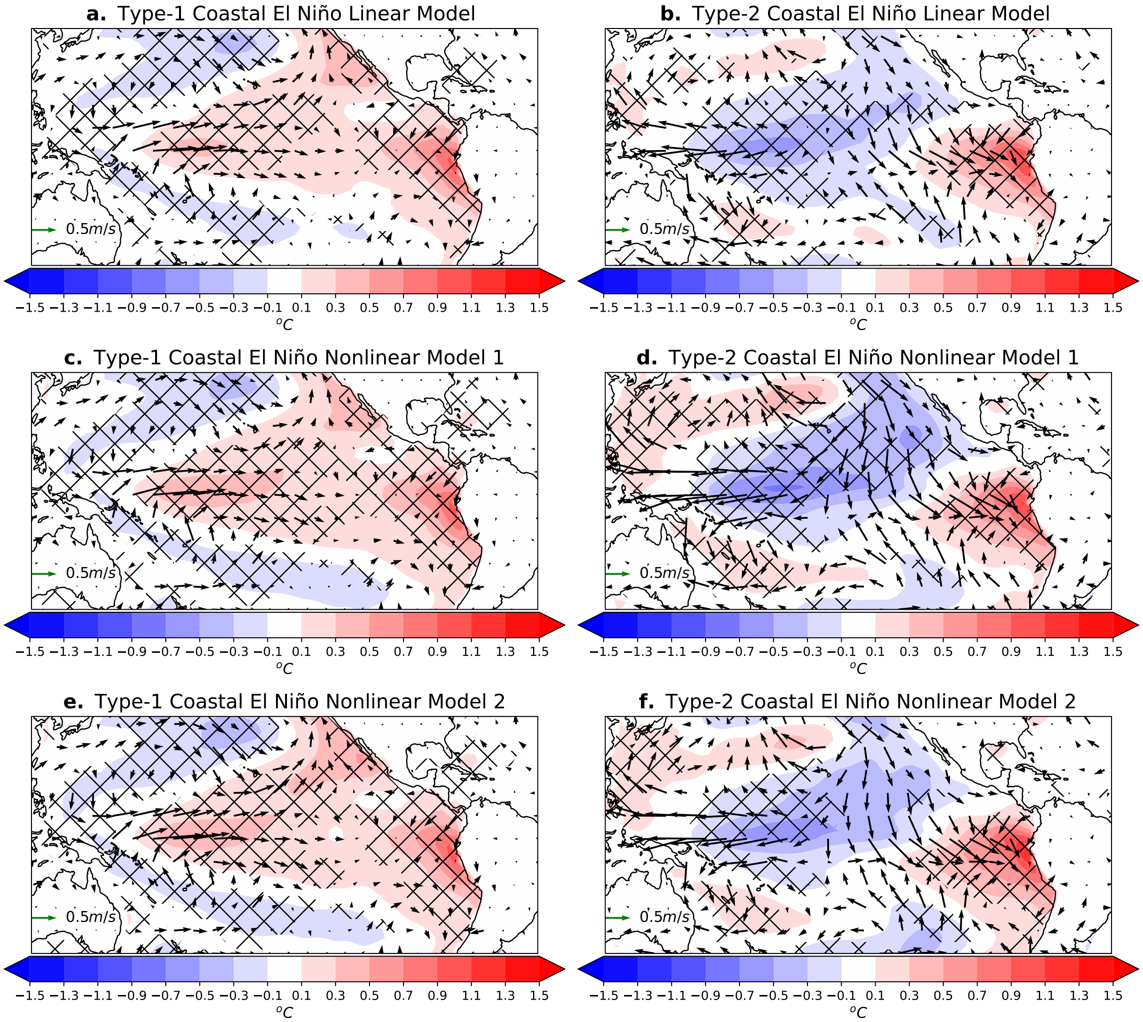

Figure S8: **Coastal El Niño composites.** Same as Figs. 4a-b, but using output from a **a.**, **b.** linear inverse model simulation (100,000yr), and **c.**, **d.** a nonlinear inverse model simulation without interacting terms (100,000yr) (see Text S1). Figs. 4a-b are repeated in **e.**, **f.** for the reader's convenience.

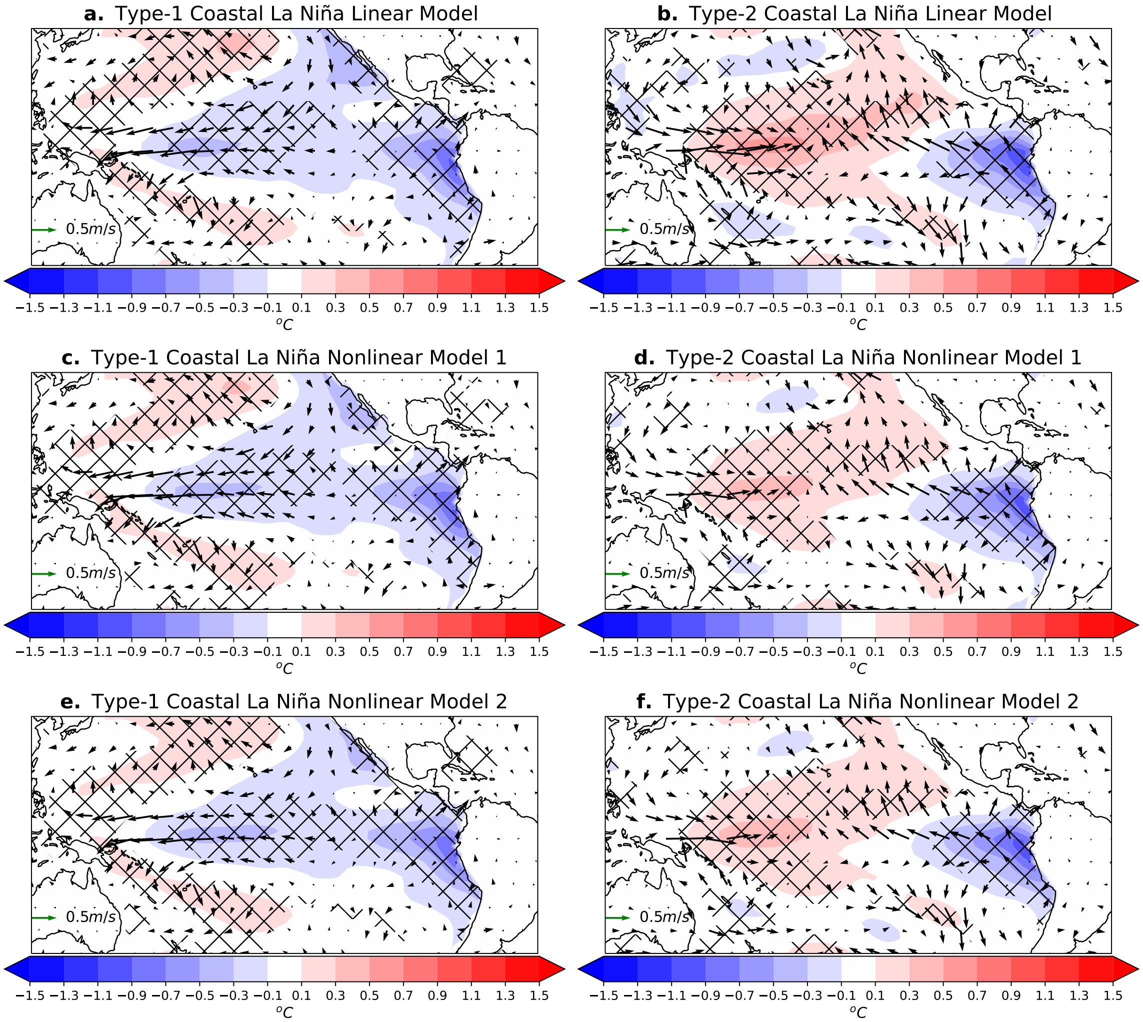

Figure S9: **Coastal La Niña composites.** Same as Figs. 4c-d, but using output from a **a.**, **b.** linear inverse model simulation (100,000yr), and **c.**, **d.** a nonlinear inverse model simulation without interacting terms (100,000yr) (see Text S1). Figs. 4c-d are repeated in **e.**, **f.** for the reader's convenience.

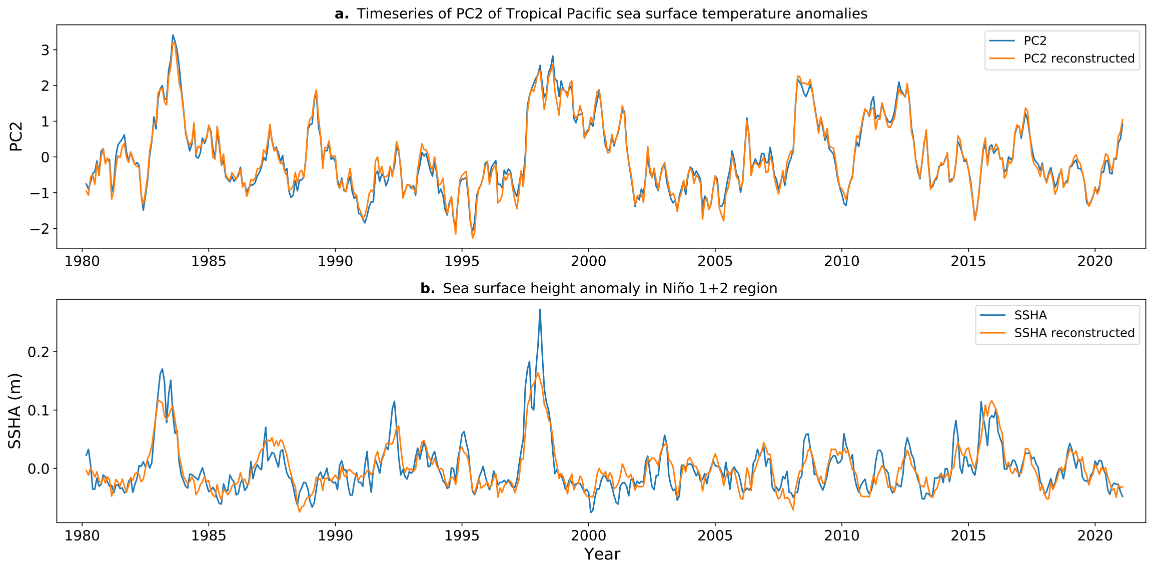

Figure S10: Observed (blue) and offline reconstructed (orange; see Methods) timeseries of **a.** PC2 of Tropical Pacific sea surface temperature anomalies, and **b.** sea surface height anomalies (SSHA) in the Niño 1+2 region. The correlation coefficients between observed and reconstructed timeseries are 0.98 and 0.88 respectively.

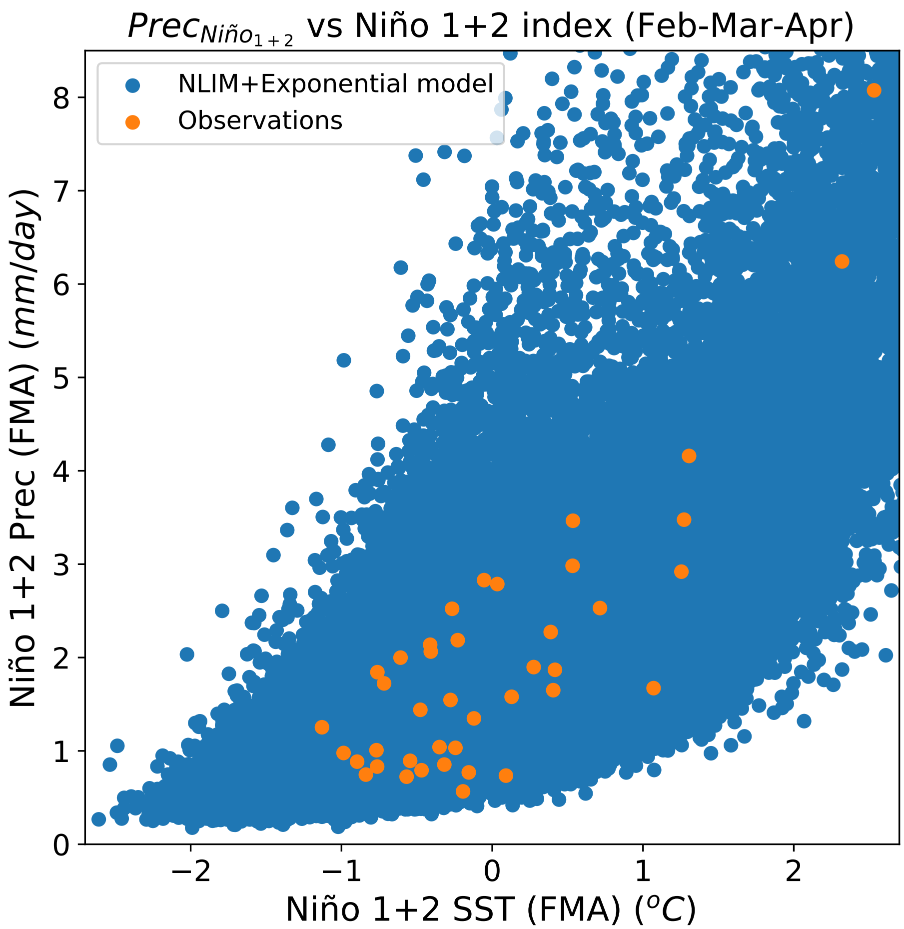

Figure S11: Scatterplot between Niño 1+2 index and mean precipitation over the Niño 1+2 region during Feb-Mar-Apr. Orange represents values in observations (1980-2020) and blue values simulated by the exponential precipitation model applied to the nonlinear inverse model output.